

# A new mixed potential representation for the equations of unsteady, incompressible flow

Leslie Greengard\*      Shidong Jiang†

September 28, 2018

## Abstract

We present a new integral representation for the unsteady, incompressible Stokes or Navier-Stokes equations, based on a linear combination of heat and harmonic potentials. For velocity boundary conditions, this leads to a coupled system of integral equations: one for the normal component of velocity and one for the tangential components. Each individual equation is well-conditioned, and we show that using them in predictor-corrector fashion, combined with spectral deferred correction, leads to high-order accuracy solvers. The fundamental unknowns in the mixed potential representation are densities supported on the boundary of the domain. We refer to one as the *vortex source*, the other as the *pressure source* and the coupled system as the *combined source integral equation*.

**Keywords:** Unsteady Stokes flow, Navier-Stokes equations, boundary integral equations, heat potentials, harmonic potentials, predictor corrector method, mixed potential formulation, spectral deferred correction method.

---

\*Courant Institute of Mathematical Sciences, New York University, New York, New York 10012 and Flatiron Institute, Simons Foundation, New York, New York 10010. (Email: greengard@courant.nyu.edu).

†Department of Mathematical Sciences, New Jersey Institute of Technology, Newark, New Jersey 07102 This work was supported in part by the NSF under grant DMS-1720405 and by the Flatiron Institute, a division of the Simons Foundation. (Email: shidong.jiang@njit.edu).

## 1 Introduction

We present a new integral representation for the numerical solution of the unsteady, incompressible Navier-Stokes equations:

$$\frac{\partial \mathbf{u}}{\partial t} = \nu \Delta \mathbf{u} - \nabla p - (\mathbf{u} \cdot \nabla) \mathbf{u} + \mathbf{f}, \quad \nabla \cdot \mathbf{u} = 0, \quad (1)$$

or their linearization, the unsteady Stokes equations,

$$\frac{\partial \mathbf{u}}{\partial t} = \nu \Delta \mathbf{u} - \nabla p + \mathbf{F}, \quad \nabla \cdot \mathbf{u} = 0. \quad (2)$$

The domain, which may be non-stationary, will be denoted at time  $t \in [0, T]$  by  $D(t)$  with boundary  $\Gamma(t)$ . The entire space-time domain will be denoted by  $D_T$  with boundary  $\Gamma_T$ . Here,  $\mathbf{u}(\mathbf{x}, t)$  is the velocity field of interest,  $\nu$  is the viscosity, and  $p(\mathbf{x}, t)$  is the pressure at a point  $\mathbf{x} \in D(t)$ . In eqs. (1) and (2),  $\mathbf{f}$  and  $\mathbf{F}$  are forcing terms. Initial conditions for the velocity are given by

$$\mathbf{u}(\mathbf{x}, 0) = \mathbf{u}_0(\mathbf{x}), \quad \mathbf{x} \in D(0), \quad (3)$$

and we restrict our attention to the case where “velocity” boundary conditions are prescribed:

$$\mathbf{u}(\mathbf{x}, t) = \mathbf{g}(\mathbf{x}, t), \quad (\mathbf{x}, t) \in \Gamma_T. \quad (4)$$

In this paper, we focus on the linearized problem, assuming that  $\mathbf{F}$  is known. From a numerical perspective, it already contains the essential difficulty faced by marching schemes for the Navier-Stokes equations, which usually treat the nonlinear, advective term explicitly. That essential difficulty concerns computing the evolution of a diffusing velocity field, while maintaining the incompressibility condition

$$\nabla \cdot \mathbf{u} = 0 \quad (5)$$

through the addition of a pressure gradient.

Beginning with the work of Chorin and Temam [12, 49], one of the most popular approaches for solving this problem is through the use of fractional step “projection” methods. A simple version of such a scheme involves first solving a diffusion equation for the velocity field with an explicit approximation of  $\nabla p$  and  $\mathbf{F}$ , followed by the solution of a Poisson equation for the pressure to enforce the incompressibility constraint. Several decisions must be made in such schemes, including the choice of boundary conditions

for the diffusion step and the choice of boundary conditions for the pressure correction/projection step. We do not seek to review the literature here and refer the reader to [9, 31, 40] for additional references and a more thorough discussion.

To avoid fractional steps, an alternative is to use a gauge method. Rather than solving the unsteady Stokes equations directly, one solves a system of the form:

$$\begin{aligned}\frac{\partial \mathbf{m}}{\partial t} &= \nu \Delta \mathbf{m} + \mathbf{F}, \\ \Delta \phi &= \nabla \cdot \mathbf{m},\end{aligned}\tag{6}$$

from which one obtains  $\mathbf{u}$  and  $p$  as

$$\begin{aligned}\mathbf{u} &= \mathbf{m} - \nabla \phi, \\ p &= \phi_t - \nu \Delta \phi.\end{aligned}$$

Such schemes require suitable boundary conditions for  $\phi$  and  $\mathbf{m}$ , but avoid the fractional step and are more straightforward to discretize with high order accuracy in time (see, for example, [10, 14, 19, 46, 51]).

One can also obtain an unconstrained formulation by taking the curl of the unsteady Stokes equations, yielding an equation for the evolution of vorticity  $\boldsymbol{\omega} = \nabla \times \mathbf{u}$ . In three dimensions, we have

$$\frac{\partial \boldsymbol{\omega}}{\partial t} = \nu \Delta \boldsymbol{\omega} + \nabla \times \mathbf{F},\tag{7}$$

while in two dimensions,

$$\frac{\partial \omega}{\partial t} = \nu \Delta \omega + \left( \frac{\partial F_2}{\partial x_1} - \frac{\partial F_1}{\partial x_2} \right).\tag{8}$$

Here,  $\mathbf{u} = (u_1, u_2)$ ,  $\mathbf{F} = (F_1, F_2)$ , and vorticity is the scalar  $\omega = \frac{\partial u_2}{\partial x_1} - \frac{\partial u_1}{\partial x_2}$ . This approach is particularly natural in the two-dimensional setting, where one can introduce a scalar stream function  $\Psi$ , with

$$\mathbf{u} = \nabla^\perp \Psi = \left( \frac{\partial \Psi}{\partial x_2}, -\frac{\partial \Psi}{\partial x_1} \right),\tag{9}$$

so that the incompressibility constraint is automatically satisfied. It is easy to see that the stream function must satisfy the Poisson equation

$$\Delta \Psi = -\omega.\tag{10}$$

A major difficulty with this approach is that the boundary conditions for vorticity are nonlocal [2, 5, 15, 17, 45]. Instead, one can also formulate

the two-dimensional Navier-Stokes equations entirely in terms of the stream function [4, 24, 32, 33]:

$$\frac{\partial \Delta \Psi}{\partial t} = \nu \Delta^2 \Psi - \left( \frac{\partial F_2}{\partial x_1} - \frac{\partial F_1}{\partial x_2} \right). \quad (11)$$

Since this is a fourth order partial differential equation, one can directly impose velocity boundary conditions by specifying  $\nabla^\perp \Psi$  on  $\Gamma(t)$ . Unfortunately, the extension of this approach to three dimensions is much more complicated (see, for example, [18]).

Finally, we should note that there is a Green's function for the linearized equations (2), called the *unsteady Stokeslet*. In [34], integral equation methods were proposed using the corresponding layer potentials. While effective, they are somewhat complicated to implement with existing fast algorithms and high-order accurate quadrature methods. We will return to this point in the concluding section.

Here, we propose a new integral representation for the solution of the unsteady Stokes equations that is divergence-free by construction, involves only the use of harmonic and heat potentials, permits the natural imposition of velocity boundary conditions, and is applicable in either two or three dimensions. Since fast and high-order algorithms have been created for harmonic and heat potentials over the past several decades, powerful numerical machinery can immediately be brought to bear. The heart of our approach is to find a particular solution to the inhomogeneous equation (accounting for the forcing term  $\mathbf{F}$ ), followed by a solution of the homogeneous, unsteady Stokes problem to enforce the desired boundary conditions. In three dimensions, the latter step involves a representation of the solution of the form

$$\begin{aligned} \mathbf{u}(\mathbf{x}, t) &= \nabla \phi(\mathbf{x}, t) + \nabla \times \mathbf{K}(\mathbf{x}, t), \\ p(\mathbf{x}, t) &= -\phi_t(\mathbf{x}, t), \end{aligned}$$

where  $\phi$  is harmonic and  $\mathbf{K}$  satisfies the vector homogeneous heat equation. Both  $\phi$  and  $\mathbf{K}$  will be defined in terms of layer potentials on  $\Gamma_T$ , whose source densities will be referred to as the pressure source and vortex source, respectively. Enforcing velocity boundary conditions will lead to the *combined source integral equation*.

The paper is organized as follows. In section 2, we briefly summarize the necessary mathematical background. In section 3, we discuss the mixed potential representation and derive the combined source integral equation. In section 4, we compute the spectrum and condition number of a fully implicit version of the combined source integral equations and in section 5,

we present numerical experiments. In section 6, we investigate a kind of predictor-corrector scheme, where we impose the normal and tangential boundary conditions sequentially. In section 7, we show how high-order accuracy can be achieved using a spectral deferred correction scheme. We conclude with an outline of future work.

**Remark 1** *For the sake of simplicity, we assume that  $\nu = 1$  in the remainder of this paper. This is easily accomplished in the unsteady Stokes equations by rescaling the time variable.*

## 2 Analytical Preliminaries

For a fixed Lipschitz domain  $D$  in  $\mathbb{R}^d$  with boundary  $\Gamma$ , we let  $L^2(D)$  denote the space of all square integrable functions in  $D$  and we let  $L^2(\Gamma)$  denote the space of all square integrable functions on  $\Gamma$ . For the time-varying space-time cylinder  $D_T \subset \mathbb{R}^d \times [0, T]$  with boundary  $\Gamma_T$ , we let  $L^2(D_T)$  denote the space of all square integrable functions in  $D_T$  and we let  $L^2(\Gamma_T)$  denote the space of all square integrable functions on  $\Gamma_T$ . We briefly summarize the necessary aspects of classical potential theory for the Laplace and heat equations in  $\mathbb{R}^d$  ( $d = 2, 3$ ).

### 2.1 Harmonic potentials

The Green's function for the Laplace equation in free space is given by

$$G_L(\mathbf{x}, \mathbf{y}) = \begin{cases} -\frac{1}{2\pi} \ln |\mathbf{x} - \mathbf{y}| & \text{in } \mathbb{R}^2, \\ \frac{1}{4\pi |\mathbf{x} - \mathbf{y}|} & \text{in } \mathbb{R}^3. \end{cases} \quad (12)$$

**Definition 1** *Let  $\mathbf{x} \in \mathbb{R}^d$ . The single layer potential  $\mathcal{S}_L$  with density  $\rho \in L^2(\Gamma)$  is defined by*

$$\mathcal{S}_L[\rho](\mathbf{x}) = \int_{\Gamma} G_L(\mathbf{x}, \mathbf{y}) \rho(\mathbf{y}) ds(\mathbf{y}). \quad (13)$$

*The volume potential  $\mathcal{V}_L$  with density  $f \in L^2(D)$  is defined by*

$$\mathcal{V}_L[f](\mathbf{x}) = \int_D G_L(\mathbf{x}, \mathbf{y}) f(\mathbf{y}) dy. \quad (14)$$

### 2.1.1 Jump relations

For  $\mathbf{x}_0 \in \Gamma$ , the normal derivative of the single layer potential  $\mathcal{S}_L[\rho]$  satisfies the jump relation

$$\lim_{\epsilon \rightarrow 0^+} \frac{\partial \mathcal{S}_L[\rho](\mathbf{x}_0 \pm \epsilon \nu(\mathbf{x}_0))}{\partial \nu(\mathbf{x}_0)} = \mp \frac{1}{2} \rho(\mathbf{x}_0) + \mathcal{S}_{L\nu}[\rho](\mathbf{x}_0), \quad (15)$$

where  $\nu(\mathbf{x}_0)$  is the unit outward normal vector to  $\Gamma$  at the boundary point  $\mathbf{x}_0$  and

$$\mathcal{S}_{L\nu}[\rho](\mathbf{x}_0) = \text{p.v.} \int_{\Gamma} \frac{\partial G_L(\mathbf{x}_0, \mathbf{y})}{\partial \nu(\mathbf{x}_0)} \rho(\mathbf{y}) ds(\mathbf{y}). \quad (16)$$

If  $D$  is a Lipschitz domain, then  $\mathcal{S}_L$  is a compact operator on  $L^2(\Gamma)$  and  $\mathcal{S}_{L\nu}^*$  is bounded. The latter is compact when  $\Gamma$  is  $C^1$  [21, 50].

### 2.1.2 Tangential derivatives

In two dimensions, the tangential derivative of the single layer potential is denoted by

$$\mathcal{S}_{L\tau}[\rho](\mathbf{x}_0) = \int_{\Gamma} \frac{\partial G_L(\mathbf{x}_0, \mathbf{y})}{\partial \tau(\mathbf{x}_0)} \rho(\mathbf{y}) ds(\mathbf{y}), \quad (17)$$

where  $\tau(\mathbf{x}_0)$  is the unit tangential vector at  $\mathbf{x}_0 \in \Gamma$ .  $\mathcal{S}_{L\tau}$  is defined in the Cauchy principal value sense and is a bounded operator on  $L^2(\Gamma)$ . In three dimensions, the tangential derivatives can be written in the form

$$\nu(\mathbf{x}_0) \times \nabla \mathcal{S}_L[\rho](\mathbf{x}_0). \quad (18)$$

This operator is, again, defined in the Cauchy principal value sense and bounded on  $L^2(\Gamma)$ .

## 2.2 Heat potentials

The Green's function for the heat equation,  $u_t = \Delta u$ , is

$$G_H(\mathbf{x}, t) = \frac{1}{(4\pi t)^{d/2}} e^{-\frac{|\mathbf{x}|^2}{4t}}, \quad \mathbf{x} \in \mathbb{R}^d. \quad (19)$$

**Definition 2** Let  $u_0 \in L^2(D(0))$ , let  $f \in L^2(D_T)$  and let  $\mu \in L^2(\Gamma_T)$ . Then, the initial heat potential  $\mathcal{I}_H$  is defined by

$$\mathcal{I}_H[u_0](\mathbf{x}, t) = \int_D G_H(\mathbf{x} - \mathbf{y}, t) u_0(\mathbf{y}) d\mathbf{y}, \quad (20)$$

the volume heat potential  $\mathcal{V}_H$  is defined by

$$\mathcal{V}_H[g](\mathbf{x}, t) = \int_0^t \int_{D(t')} G_H(\mathbf{x} - \mathbf{y}, t - t') f(\mathbf{y}, t') d\mathbf{y} dt', \quad (21)$$

and the single layer heat potential  $\mathcal{S}_H$  is defined by

$$\mathcal{S}_H[\mu](\mathbf{x}, t) = \int_0^t \int_{\Gamma(t')} G_H(\mathbf{x} - \mathbf{y}, t - t') \mu(\mathbf{y}, t') ds(\mathbf{y}) dt'. \quad (22)$$

### 2.2.1 Jump relations

It is well-known that the initial heat potential  $\mathcal{I}_H$  is a compact operator on  $L^2(D(0))$  and that the volume heat potential  $\mathcal{V}_H$  is a compact operator on  $L^2(D_T)$ . As in the harmonic case, the normal derivative of the single layer heat potential  $\mathcal{S}_{H\nu}[\mu]$  satisfies the jump relations

$$\lim_{\epsilon \rightarrow 0^+} \mathcal{S}_{H\nu}[\mu](\mathbf{x}_0 \pm \epsilon \nu(\mathbf{x}_0), t) = \mp \frac{1}{2} \mu(\mathbf{x}_0, t) + \mathcal{S}_{H\nu}[\mu](\mathbf{x}_0, t), \quad \mathbf{x}_0 \in \Gamma, \quad (23)$$

where  $\mathcal{S}_{H\nu}[\mu](\mathbf{x}_0, t)$  is the principal value of

$$\mathcal{S}_{H\nu}[\mu](\mathbf{x}_0, t) = \int_0^t \int_{\Gamma(t')} \frac{\partial G_H(\mathbf{x}_0 - \mathbf{y}, t - t')}{\partial \nu(\mathbf{x}_0)} \mu(\mathbf{y}, t') ds(\mathbf{y}) dt'.$$

In two dimensions, the tangential derivative of the single layer heat potential is denoted by

$$\mathcal{S}_{H\tau}[\mu](\mathbf{x}_0, t) = \int_0^t \int_{\Gamma(t')} \frac{\partial G_H(\mathbf{x}_0 - \mathbf{y}, t - t')}{\partial \tau(\mathbf{x}_0)} \mu(\mathbf{y}, t') ds(\mathbf{y}) dt', \quad (24)$$

where  $\tau(\mathbf{x}_0)$  is the unit tangential vector at  $\mathbf{x}_0 \in \Gamma$ .  $\mathcal{S}_{H\tau}$  is defined in the Cauchy principal value sense and is a bounded operator on  $L^2(\Gamma)$ .

### 2.2.2 The vector heat potential

In three dimensions, we will also make use of a vector heat potential, defined by

$$\mathbf{K}_H[\mathbf{J}](\mathbf{x}, t) = \int_0^t \int_{\Gamma(t')} G_H(\mathbf{x} - \mathbf{y}, t - t') \mathbf{J}(\mathbf{y}, t') ds(\mathbf{y}) dt', \quad (25)$$

where  $\mathbf{J}$  is a tangential vector field on  $\Gamma$ .

**Definition 3** For reasons that will become clear below, we will refer to  $\mathbf{J}$  or  $\mu$  as the vortex source. ( $\mathbf{K}_H[\mathbf{J}]$  will play a role analogous to that of the vector potential in electromagnetic theory, where the source is a surface electric current.)

It is straightforward to verify that, as in the electromagnetic case, the tangential components of  $\nabla \times \mathbf{K}_H[\mathbf{J}]$  are given by [13]:

$$\lim_{\epsilon \rightarrow 0^+} \nu(\mathbf{x}_0) \times (\nabla \times \mathbf{K}_H)[\mathbf{J}](\mathbf{x}_0 \pm \epsilon \nu(\mathbf{x}_0), t) = \pm \frac{1}{2} \mathbf{J}(\mathbf{x}_0, t) + \mathbf{M}_H[\mathbf{J}](\mathbf{x}_0, t), \quad (26)$$

where

$$\mathbf{M}_H[\mathbf{J}](\mathbf{x}_0, t) = \nu(\mathbf{x}_0) \times (\nabla \times \mathbf{K}_H)[\mathbf{J}](\mathbf{x}_0, t), \quad \mathbf{x}_0 \in \Gamma, \quad (27)$$

interpreted in the principal value sense.  $\mathbf{M}_H[\mathbf{J}]$  is a compact operator when  $\Gamma$  is  $C^1$  [13]. Finally,

$$\nu(\mathbf{x}_0) \cdot \nabla \times \mathbf{K}_H[\mathbf{J}](\mathbf{x}_0, t) \quad (28)$$

is defined in the Cauchy principal value sense, continuous across the boundary of  $\Gamma \in C^1$ , and bounded on  $L^2(\Gamma)$ .

### 2.3 The Helmholtz decomposition of a vector field

Let  $D \subset \mathbb{R}^d$  be a bounded Lipschitz domain ( $d = 2, 3$ ). It is well-known [23] that every vector field  $\mathbf{F} \in L^2(D)$  has a decomposition of the form

$$\mathbf{F} = \nabla \phi + \mathbf{w}, \quad (29)$$

where  $\mathbf{w}$  is divergence-free (or *solenoidal*) and  $\nabla \phi$  is curl-free (or *irrotational*). We will sometimes write

$$\mathbf{F} = \mathbf{F}_G + \mathbf{F}_S \quad (30)$$

instead of (29), where  $\mathbf{F}_G$  is irrotational and  $\mathbf{F}_S$  is solenoidal.

Without boundary conditions on  $\mathbf{w}$  or  $\phi$ , the Helmholtz decomposition is not unique. Nevertheless, assuming  $\mathbf{F}$  is sufficiently smooth, a simple explicit construction is easily computed.

**Lemma 1** [3] Let  $\mathbf{F}$  be a twice differentiable vector field in a domain  $D$  with boundary  $\Gamma$  in  $\mathbb{R}^3$ , and let

$$\phi(\mathbf{x}) = - \int_D G_L(\mathbf{x} - \mathbf{y}) (\nabla_{\mathbf{y}} \cdot \mathbf{F}(\mathbf{y})) \, d\mathbf{y} + \int_{\Gamma} G_L(\mathbf{x} - \mathbf{y}) (\nu(\mathbf{y}) \cdot \mathbf{F}(\mathbf{y})) \, ds(\mathbf{y}),$$



$$\mathbf{A}(\mathbf{x}) = \int_D G_L(\mathbf{x} - \mathbf{y}) (\nabla_{\mathbf{y}} \times \mathbf{F}(\mathbf{y})) d\mathbf{y} - \int_{\Gamma} G_L(\mathbf{x} - \mathbf{y}) (\nu(\mathbf{y}) \times \mathbf{F}(\mathbf{y})) ds(\mathbf{y}).$$

Then

$$\mathbf{F} = \nabla \times \mathbf{A} + \nabla \phi.$$

In  $\mathbb{R}^2$ , if  $\mathbf{F} = (F_1, F_2)$  is twice differentiable in a domain  $D$  with boundary  $\Gamma$ , let  $\phi$  be defined as above and let

$$\psi(\mathbf{x}) = \int_D G_L(\mathbf{x} - \mathbf{y}) \left( \nabla_{\mathbf{y}}^{\perp} \cdot \mathbf{F}(\mathbf{y}) \right) d\mathbf{y} - \int_{\Gamma} G_L(\mathbf{x} - \mathbf{y}) (\tau(\mathbf{y}) \cdot \mathbf{F}(\mathbf{y})) ds(\mathbf{y}),$$

where  $\nabla_{\mathbf{x}}^{\perp} \cdot \mathbf{F}(\mathbf{x}) = \frac{\partial F_2}{\partial x_1} - \frac{\partial F_1}{\partial x_2}$  and  $\tau$  denotes the unit tangent vector along  $\Gamma$ . Then

$$\mathbf{F} = \nabla^{\perp} \psi + \nabla \phi.$$

Using the notation above, we can write this more compactly as

$$\begin{aligned} \phi(\mathbf{x}) &= -\mathcal{V}_L[\nabla \cdot \mathbf{F}](\mathbf{x}) + \mathcal{S}_L[\nu \cdot \mathbf{F}](\mathbf{x}). \\ \mathbf{A}(\mathbf{x}) &= \mathcal{V}_L[\nabla \times \mathbf{F}](\mathbf{x}) - \mathcal{S}_L[\nu \times \mathbf{F}](\mathbf{x}). \\ \psi(\mathbf{x}) &= \mathcal{V}_L[\nabla^{\perp} \cdot \mathbf{F}](\mathbf{x}) - \mathcal{S}_L[\tau \cdot \mathbf{F}](\mathbf{x}). \end{aligned} \tag{31}$$

Both the harmonic volume potentials and the harmonic single layer potentials can be computed in optimal time, and with high order accuracy, using the fast multipole method and suitable quadrature rules [8, 11, 20, 25, 27, 30, 38, 42, 47].

**Remark 2** In free space, there is an even simpler construction for the Helmholtz decomposition (assuming sufficiently rapid decay of  $\mathbf{F}$ ).

**Lemma 2** [37] If  $\mathbf{F} \in L^2(\mathbb{R}^d)$ , then

$$\mathbf{F}_G = -\nabla \left( \nabla \cdot \int_{\mathbb{R}^d} G_L(\mathbf{x} - \mathbf{y}) \mathbf{F}(\mathbf{y}) d\mathbf{y} \right), \quad \mathbf{F}_S = \mathbf{F} - \mathbf{F}_G,$$

where  $G_L$  is the Green's function for the Laplace equation.

### 3 Potential theory for the unsteady Stokes equations

Before turning to the full boundary value problem, it is worth stating a fundamental, but rarely used, fact about the unsteady Stokes equations in the absence of physical boundaries.

**Lemma 3** ([37], chapter 4) *Let  $\mathbf{F}(\mathbf{x}, t) \in L^2(\mathbb{R}^d)$ , where  $d = 2, 3$ , with the Helmholtz decomposition*

$$\mathbf{F}(\mathbf{x}, t) = \mathbf{F}_S(\mathbf{x}, t) + \mathbf{F}_G(\mathbf{x}, t),$$

where  $\mathbf{F}_S$  is solenoidal and  $\mathbf{F}_G$  is irrotational. Then the solution to (2) in  $\mathbb{R}^d$  with divergence-free initial data  $\mathbf{u}_0(\mathbf{x})$  is given by

$$\begin{aligned} \mathbf{u}^{(F)}(\mathbf{x}, t) &= \mathcal{I}_H[\mathbf{u}_0](\mathbf{x}, t) + \mathcal{V}_H[\mathbf{F}_S](\mathbf{x}, t) \\ \nabla p^{(F)}(\mathbf{x}, t) &= \mathbf{F}_G(\mathbf{x}, t), \end{aligned} \quad (32)$$

where  $G_H(\mathbf{x}, t)$  is the heat kernel. (The operators  $\mathcal{I}_H$  and  $\mathcal{V}_H$  here are assumed to be defined on  $\mathbb{R}^d$  rather than a bounded domain  $D$ .)

In short, given the Helmholtz decomposition of the forcing term  $\mathbf{F}$ , the unsteady Stokes equations have an explicit solution in free space by quadrature. This turns out to be true in a bounded domain as well.

**Lemma 4** *Let  $\mathbf{F}(\mathbf{x}, t) \in L^2(D)$ , where  $d = 2, 3$ , with the Helmholtz decomposition*

$$\mathbf{F}(\mathbf{x}, t) = \mathbf{F}_S(\mathbf{x}, t) + \nabla\phi(\mathbf{x}, t),$$

where  $\mathbf{F}_S = \nabla \times \mathbf{A}$  in  $\mathbb{R}^3$  and  $\mathbf{F}_S = \nabla^\perp \psi$  in  $\mathbb{R}^2$ . Then, a particular solution to eqs. (2) and (3) is given by

$$\begin{aligned} \mathbf{u}^{(F)}(\mathbf{x}, t) &= \mathcal{I}_H[\mathbf{u}_0](\mathbf{x}, t) + \nabla \times \mathcal{V}_H[\mathbf{A}](\mathbf{x}, t) && \text{in } \mathbb{R}^3 \\ \nabla p^{(F)}(\mathbf{x}, t) &= \nabla\phi(\mathbf{x}, t), \\ \mathbf{u}^{(F)}(\mathbf{x}, t) &= \mathcal{I}_H[\mathbf{u}_0](\mathbf{x}, t) + \nabla^\perp \mathcal{V}_H[\psi](\mathbf{x}, t) && \text{in } \mathbb{R}^2 \\ \nabla p^{(F)}(\mathbf{x}, t) &= \nabla\phi(\mathbf{x}, t), \end{aligned} \quad (33)$$

where the initial and volume heat potentials are given in definition 2.

*Proof:* It is straightforward to verify that the partial differential equation (2) is satisfied. The fact that  $\mathbf{u}^{(F)}(\mathbf{x}, t)$  is divergence-free follows immediately from lemma 3 for the term  $\mathcal{I}_H[\mathbf{u}_0](\mathbf{x}, t)$  and by construction for the term involving  $\mathcal{V}_H[\mathbf{A}](\mathbf{x}, t)$  or  $\mathcal{V}_H[\psi](\mathbf{x}, t)$ .  $\square$

Thus, from the preceding Lemma, we may represent the solution to the full unsteady Stokes equations in the form

$$\mathbf{u} = \mathbf{u}^{(F)} + \mathbf{u}^{(B)}, \quad \nabla p = \nabla p^{(F)} + \nabla p^{(B)},$$

where  $(\mathbf{u}^{(B)}, \nabla p^{(B)})$  satisfy the homogeneous, linearized equations

$$\begin{aligned} \frac{\partial \mathbf{u}^{(B)}}{\partial t} &= \Delta \mathbf{u}^{(B)} - \nabla p^{(B)}, & (\mathbf{x}, t) \in D_T, \\ \nabla \cdot \mathbf{u}^{(B)} &= 0, & (\mathbf{x}, t) \in D_T, \\ \mathbf{u}^{(B)}(\mathbf{x}, 0) &= \mathbf{0}, & \mathbf{x} \in D(0), \\ \mathbf{u}^{(B)}(\mathbf{x}, t) &= \tilde{\mathbf{g}}(\mathbf{x}, t) := \mathbf{g}(\mathbf{x}, t) - \mathbf{u}^{(F)}(\mathbf{x}, t), & (\mathbf{x}, t) \in \Gamma_T. \end{aligned} \quad (34)$$

There is a significant advantage in solving the homogeneous equations (34) rather than eqs. (2) to (4), as we shall now see.

### 3.1 The mixed potential representation

Let us represent the solution to the homogeneous system,

$$(\mathbf{u}^{(B)}(\mathbf{x}, t), p^{(B)}(\mathbf{x}, t)),$$

in terms of harmonic and heat layer potentials. In three dimensions, we define

$$\begin{aligned} \mathbf{u}^{(B)}(\mathbf{x}, t) &= \nabla \mathcal{S}_L[\rho](\mathbf{x}, t) + \nabla \times \mathbf{K}_H[\mathbf{J}](\mathbf{x}, t), \\ p^{(B)}(\mathbf{x}, t) &= -\frac{\partial}{\partial t} \mathcal{S}_L[\rho](\mathbf{x}, t), \end{aligned} \quad (35)$$

while in two dimensions, we define

$$\begin{aligned} \mathbf{u}^{(B)}(\mathbf{x}, t) &= \nabla \mathcal{S}_L[\rho](\mathbf{x}, t) + \nabla^\perp \mathcal{S}_H[\mu](\mathbf{x}, t), \\ p^{(B)}(\mathbf{x}, t) &= -\frac{\partial}{\partial t} \mathcal{S}_L[\rho](\mathbf{x}, t). \end{aligned} \quad (36)$$

Here,  $\rho$ ,  $\mathbf{J}$  and  $\mu$  are unknown *boundary densities* to be determined. It is straightforward to verify that the representations (35) and (36) satisfy the first three equations in (34).

**Definition 4** *Because of the preceding relations, we will refer to  $\rho$  as the pressure source or pressure source density.*

#### 3.1.1 The combined source integral equation

If we decompose the velocity field into a sum of normal and tangential components on the boundary, then imposing velocity boundary conditions

leads, in two dimensions, to the system of integral equations

$$\begin{aligned} \frac{1}{2}\rho(\mathbf{x}, t) + \mathcal{S}_{L\nu}[\rho](\mathbf{x}, t) + \mathcal{S}_{H\tau}[\mu](\mathbf{x}, t) &= \nu \cdot \tilde{\mathbf{g}}(\mathbf{x}, t), \\ \frac{1}{2}\mu(\mathbf{x}, t) + \mathcal{S}_{H\nu}[\mu](\mathbf{x}, t) - \mathcal{S}_{L\tau}[\rho](\mathbf{x}, t) &= -\tau \cdot \tilde{\mathbf{g}}(\mathbf{x}, t) \end{aligned} \quad (37)$$

for the unknowns  $\rho$  and  $\mu$ , where  $\mathbf{x}$  is a point on the boundary  $\Gamma(t)$ .

In three dimensions, we obtain system of integral equations

$$\begin{aligned} \frac{1}{2}\rho(\mathbf{x}, t) + \mathcal{S}_{L\nu}[\rho](\mathbf{x}, t) + \nu(\mathbf{x}, t) \cdot \nabla \times \mathbf{K}_H[\mathbf{J}](\mathbf{x}, t) &= \nu(\mathbf{x}, t) \cdot \tilde{\mathbf{g}}(\mathbf{x}, t), \\ \frac{1}{2}\mathbf{J}(\mathbf{x}, t) + \mathbf{M}_H[\mathbf{J}](\mathbf{x}, t) + \nu(\mathbf{x}, t) \times \nabla \mathcal{S}_L[\rho](\mathbf{x}, t) &= \nu(\mathbf{x}, t) \times \tilde{\mathbf{g}}(\mathbf{x}, t). \end{aligned} \quad (38)$$

for the unknowns  $\rho$  and  $\mathbf{J}$ , where  $\mathbf{x}$  is a point on the boundary  $\Gamma(t)$ . We will refer to either (37) or (38) as the *combined source integral equation*.

One major advantage of the mixed potential representation is that the unknown densities (the pressure source and the vortex source) correspond to physical quantities of interest. The harmonic potential  $\phi(\mathbf{x}, t) = \mathcal{S}_L[\rho](\mathbf{x}, t)$  determines the pressure, according to eqs. (35) and (36), while the heat potentials determine the vorticity. More precisely, in three dimensions,

$$\omega(\mathbf{x}, t) = \nabla \times (\nabla \times \mathbf{K}_H)[\mathbf{J}](\mathbf{x}, t) + \nabla \times \mathbf{u}^{(F)},$$

while in two dimensions,

$$\omega(\mathbf{x}, t) = -\partial_t \mathcal{S}_H[\mu](\mathbf{x}, t) + \frac{\partial u_2^{(F)}}{\partial x_1} - \frac{\partial u_1^{(F)}}{\partial x_2},$$

where  $\mathbf{u}^{(F)} = (u_1^{(F)}, u_2^{(F)})$ . These relations may be of some direct interest in analysis.

**Remark 3** *It is, perhaps, worth noting that in the mixed potential representation, the boundary conditions for  $\mathbf{K}$  and  $\phi$  are local, but they yield exact, nonlocal expressions for the pressure and vorticity through the formulae above.*

### 3.2 Discretization

For the sake of simplicity, we restrict our attention to the integral equation system (37) in two dimensions, and begin by semi-discretization in time (i.e., discretization with respect to the time variable alone). For this, we let

$$\rho_j = \rho(\mathbf{x}, j\Delta t), \quad \mu_j = \mu(\mathbf{x}, j\Delta t).$$

$$\boldsymbol{\rho}_j = [\rho_0, \dots, \rho_j], \quad \boldsymbol{\mu}_j = [\mu_0, \dots, \mu_j]$$

We then write

$$\mathcal{S}_{\text{H}\nu}[\boldsymbol{\mu}_j](\mathbf{x}, t) = \mathcal{S}_{\text{H}\nu}^{\text{far}}[\boldsymbol{\mu}_{j-1}](\mathbf{x}, t) + \mathcal{S}_{\text{H}\nu}^{\text{loc}}[\boldsymbol{\mu}_j](\mathbf{x}, t),$$

$$\mathcal{S}_{\text{H}\tau}[\boldsymbol{\mu}_j](\mathbf{x}, t) = \mathcal{S}_{\text{H}\tau}^{\text{far}}[\boldsymbol{\mu}_{j-1}](\mathbf{x}, t) + \mathcal{S}_{\text{H}\tau}^{\text{loc}}[\boldsymbol{\mu}_j](\mathbf{x}, t),$$

to denote the semi-discrete approximations of  $\mathcal{S}_{\text{H}\nu}[\boldsymbol{\mu}]$  and  $\mathcal{S}_{\text{H}\tau}[\boldsymbol{\mu}]$ , where

$$\begin{aligned} \mathcal{S}_{\text{H}\nu}^{\text{far}}[\boldsymbol{\mu}_{j-1}](\mathbf{x}, t) &= \\ &\sum_{l=1}^{j-1} \int_{(l-1)\Delta t}^{l\Delta t} \int_{\Gamma(t')} \frac{\partial G_{\text{H}}(\mathbf{x} - \mathbf{y}, t - t')}{\partial \nu(\mathbf{x})} P_k^I[\boldsymbol{\mu}_l](\mathbf{y}, t') ds(\mathbf{y}) dt', \\ \mathcal{S}_{\text{H}\tau}^{\text{far}}[\boldsymbol{\mu}_{j-1}](\mathbf{x}, t) &= \\ &\sum_{l=1}^{j-1} \int_{(l-1)\Delta t}^{l\Delta t} \int_{\Gamma(t')} \frac{\partial G_{\text{H}}(\mathbf{x} - \mathbf{y}, t - t')}{\partial \tau(\mathbf{x})} P_k^I[\boldsymbol{\mu}_l](\mathbf{y}, t') ds(\mathbf{y}) dt', \\ \mathcal{S}_{\text{H}\nu}^{\text{loc}}[\boldsymbol{\mu}_j](\mathbf{x}, t) &= \\ &\int_{(j-1)\Delta t}^{j\Delta t} \int_{\Gamma(t')} \frac{\partial G_{\text{H}}(\mathbf{x} - \mathbf{y}, t - t')}{\partial \nu(\mathbf{x})} P_k^I[\boldsymbol{\mu}_j](\mathbf{y}, t') ds(\mathbf{y}) dt', \\ \mathcal{S}_{\text{H}\tau}^{\text{loc}}[\boldsymbol{\mu}_j](\mathbf{x}, t) &= \\ &\int_{(j-1)\Delta t}^{j\Delta t} \int_{\Gamma(t')} \frac{\partial G_{\text{H}}(\mathbf{x} - \mathbf{y}, t - t')}{\partial \tau(\mathbf{x})} P_k^I[\boldsymbol{\mu}_j](\mathbf{y}, t') ds(\mathbf{y}) dt'. \end{aligned} \tag{39}$$

Here,  $P_k^I[\boldsymbol{\mu}_l]$  is the  $k$ th order Lagrange interpolant of the data

$$\{\mu_l, \mu_{l-1}, \dots, \mu_{l-k}\}$$

at the  $(k+1)$  uniformly spaced time points  $\{l\Delta t, (l-1)\Delta t, \dots, (l-k)\Delta t\}$ .

Note that we have separated out the contributions to  $\mathcal{S}_{\text{H}\nu}$  and  $\mathcal{S}_{\text{H}\tau}$  from the early time steps ( $\mathcal{S}_{\text{H}\nu}^{\text{far}}, \mathcal{S}_{\text{H}\tau}^{\text{far}}$ ) from the contributions on the most recent time interval ( $\mathcal{S}_{\text{H}\nu}^{\text{loc}}, \mathcal{S}_{\text{H}\tau}^{\text{loc}}$ ). The superscript  $I$  in the expression  $P_k^I[\boldsymbol{\mu}_l]$  indicates that the latest time point  $t_l = l\Delta t$  is being used in the polynomial interpolant. Since  $\mathcal{S}_{\text{H}\nu}^{\text{loc}}$  and  $\mathcal{S}_{\text{H}\tau}^{\text{loc}}$  are linear operators acting on the densities  $\{\mu_j, \mu_{j-1}, \dots, \mu_{j-k}\}$ , we will also have occasion to write

$$\begin{aligned} \mathcal{S}_{\text{H}\nu}^{\text{loc}}[\boldsymbol{\mu}_j](\mathbf{x}, j\Delta t) &= \\ &\left[ A_{\text{H}\nu}^{j,k} \mu_{j-k} + \dots A_{\text{H}\nu}^{j,1} \mu_{j-1} \right] + A_{\text{H}\nu}^{j,0} \mu_j = F_{\text{H}\nu}^{j,k}[\boldsymbol{\mu}_{j-1}] + A_{\text{H}\nu}^{j,0} \mu_j \\ \mathcal{S}_{\text{H}\tau}^{\text{loc}}[\boldsymbol{\mu}_j](\mathbf{x}, j\Delta t) &= \\ &\left[ A_{\text{H}\tau}^{j,k} \mu_{j-k} + \dots A_{\text{H}\tau}^{j,1} \mu_{j-1} \right] + A_{\text{H}\tau}^{j,0} \mu_j = F_{\text{H}\tau}^{j,k}[\boldsymbol{\mu}_{j-1}] + A_{\text{H}\tau}^{j,0} \mu_j. \end{aligned} \tag{40}$$

This makes explicit the contributions of the densities at the various time steps to the local potentials  $\mathcal{S}_{H\nu}^{\text{loc}}$  and  $\mathcal{S}_{H\tau}^{\text{loc}}$ .

In the present paper, following previous work with the unsteady Stokeslet [34], we interchange the order of integration in space and time, as proposed in [39], and carry out the time integration analytically. For  $k = 1$ , using an implicit interpolation rule,  $P_1^I$ , to achieve second order accuracy in  $\Delta t$ , the kernels of the spatial operators  $A_{H\nu}^{j,0}$  and  $A_{H\tau}^{j,0}$  are

$$\begin{aligned} G_{H\nu}^{\text{loc}}(\mathbf{x}, \mathbf{y}) &= -\frac{(\mathbf{x} - \mathbf{y}) \cdot \nu}{2\pi\|\mathbf{x} - \mathbf{y}\|^2} e^{-\frac{\|\mathbf{x} - \mathbf{y}\|^2}{4\Delta t}} + \frac{(\mathbf{x} - \mathbf{y}) \cdot \nu}{8\pi\Delta t} E_1\left(\frac{\|\mathbf{x} - \mathbf{y}\|^2}{4\Delta t}\right), \\ G_{H\tau}^{\text{loc}}(\mathbf{x}, \mathbf{y}) &= -\frac{(\mathbf{x} - \mathbf{y}) \cdot \tau}{2\pi\|\mathbf{x} - \mathbf{y}\|^2} e^{-\frac{\|\mathbf{x} - \mathbf{y}\|^2}{4\Delta t}} + \frac{(\mathbf{x} - \mathbf{y}) \cdot \tau}{8\pi\Delta t} E_1\left(\frac{\|\mathbf{x} - \mathbf{y}\|^2}{4\Delta t}\right), \end{aligned} \quad (41)$$

where  $E_1(x) = \int_x^\infty \frac{e^{-t}}{t} dt$  is the exponential integral function [44].

We will have occasion to make use of the explicit form of the interpolant as well.

**Definition 5**  $P_k^E[\boldsymbol{\mu}_{j-1}](t)$  is defined to be the  $k$ th order Lagrange extrapolant of the data

$$[\mu_{j-1}, \dots, \mu_{j-(k+1)}]$$

evaluate at  $t = j\Delta t$ .

As in multistep methods for ordinary differential equations, when the interpolation order  $k > 1$ , some care is required in initialization - that is, computing the first  $k - 1$  time steps with sufficient accuracy. We will ignore this issue for the moment to avoid distractions.

Finally, the spatial integrals in  $\mathcal{S}_{H\tau}^{\text{loc}}$ ,  $\mathcal{S}_{H\nu}^{\text{loc}}$ ,  $\mathcal{S}_{L\tau}$ , and  $\mathcal{S}_{L\nu}$  involve either logarithmic singularities or principal value-type integrals. We use the quadrature schemes of [1] to discretize these integrals to sixteenth order accuracy on smooth curves.

### 3.3 History dependence and fast algorithms

From a practical perspective,  $\mathcal{S}_{H\tau}^{\text{far}}$  and  $\mathcal{S}_{H\nu}^{\text{far}}$  clearly depend on the entire space-time history of the problem at hand. In the absence of suitable algorithms, the cost of their evaluation would be prohibitive. Fortunately, a number of fast algorithms have been developed for precisely this purpose [26, 28, 41, 48] that permit their evaluation in  $O(NM \log M)$  work rather than  $O(N^2M^2)$  work, where  $N$  denotes the number of time steps and  $M$  denotes the number of points in the discretization of the boundary. We refer the reader to those papers for further details.

## 4 Spectrum of the fully implicit combined source integral equation

For the sake of simplicity, we restrict our attention to the coupled integral equations (37) in two dimensions on a stationary boundary. While at first glance, this might appear to involve a compact perturbation of the identity, that is not the case. Informally, this can be seen as follows. First, we note that the operators  $S_{L\tau}$  and  $S_{H\tau}$  are compact perturbations of the operator  $-\frac{1}{2}H$ , where  $H$  denotes the Hilbert transform operator on the circle with perimeter  $L$ .  $L$  here is the length of  $\Gamma$  [36]:

$$H[f](s) = \frac{1}{2\pi} p.v. \int_0^L \cot\left(\frac{\pi(s-s')}{L}\right) f(s') ds'.$$

Thus, the system can be written in the form

$$\begin{bmatrix} \frac{1}{2}I & \frac{1}{2}H \\ -\frac{1}{2}H & \frac{1}{2}I \end{bmatrix} \begin{bmatrix} \rho \\ \mu \end{bmatrix} + \mathbf{C} \begin{bmatrix} \rho \\ \mu \end{bmatrix} = \begin{bmatrix} \nu \cdot \tilde{\mathbf{g}}(\mathbf{x}, t) \\ -\tau \cdot \tilde{\mathbf{g}}(\mathbf{x}, t) \end{bmatrix}, \quad (42)$$

where  $\mathbf{C}$  is compact. Since  $H^2 = -I$ , the determinant of the leading part of the system vanishes, so that the coupled system fails to be a Fredholm equation of the second kind.

We now study the spectrum of the integral equation in detail when  $\Gamma$  is a circle of radius  $r$ . The resulting properties follow qualitatively for any smooth curve. More specifically, let us assume we are using a second-order accurate one-step implicit marching scheme, as described in section 3.2. This yields an integral equation at the  $j$ th time step of the form

$$\begin{bmatrix} \frac{1}{2}I + \mathcal{S}_{L\nu} & A_{H\tau}^{j,0} \\ -\mathcal{S}_{L\tau} & \frac{1}{2}I + A_{H\nu}^{j,0} \end{bmatrix} \begin{bmatrix} \rho_j \\ \mu_j \end{bmatrix} = \begin{bmatrix} \nu \cdot \tilde{\mathbf{g}} - \mathcal{S}_{H\tau}^{\text{far}}[\boldsymbol{\mu}_{j-1}] - F_{H\tau}^{j,1}[\boldsymbol{\mu}_{j-1}] \\ -\tau \cdot \tilde{\mathbf{g}} - \mathcal{S}_{H\nu}^{\text{far}}[\boldsymbol{\mu}_{j-1}] - F_{H\nu}^{j,1}[\boldsymbol{\mu}_{j-1}] \end{bmatrix} \quad (43)$$

using the notation of section 3.2.

The kernels of the operators on the left-hand side of (43) are given by

$$G_{L\nu}(\mathbf{x}, \mathbf{y}) = -\frac{(\mathbf{x} - \mathbf{y}) \cdot \nu}{2\pi \|\mathbf{x} - \mathbf{y}\|^2}, \quad G_{L\tau}(\mathbf{x}, \mathbf{y}) = -\frac{(\mathbf{x} - \mathbf{y}) \cdot \tau}{2\pi \|\mathbf{x} - \mathbf{y}\|^2} \quad (44)$$

and (41). On a circle of radius  $r$ , we have

$$\begin{aligned} \mathbf{x} &= (r \cos s', r \sin s'), & \mathbf{y} &= (r \cos s, r \sin s) \\ (\mathbf{x} - \mathbf{y}) \cdot \nu &= r(1 - \cos(s' - s)), & (\mathbf{x} - \mathbf{y}) \cdot \tau &= r \sin(s' - s), \\ \|\mathbf{x} - \mathbf{y}\|^2 &= 2r^2(1 - \cos(s' - s)). \end{aligned}$$

We then have

$$G_{L\nu}(\mathbf{x}, \mathbf{y}) = -\frac{1}{4\pi r}, \quad G_{L\tau}(\mathbf{x}, \mathbf{y}) = -\frac{1}{4\pi r} \cot\left(\frac{s' - s}{2}\right). \quad (45)$$

That is, the kernel of  $S_{L\nu}$  is constant and  $S_{L\tau} = -\frac{1}{2}H$  where  $H$  is the Hilbert transform on the unit circle. It is easy to verify that all of these operators are diagonalized by the Fourier transform. Thus, we only need to consider the  $2 \times 2$  block for each Fourier mode  $e^{iks}$  with  $k \in \mathbb{Z}$ .

For  $k = 0$ , we have

$$\begin{aligned} \left(\frac{1}{2}I + S_{L\nu}\right)[1] &= \frac{1}{2} - \frac{1}{4\pi r} \int_0^{2\pi} 1 \cdot r ds = 0, \\ S_{L\tau}[1] &= -\frac{1}{2}H[1] = 0, \end{aligned} \quad (46)$$

$A_{H\tau}^{j,0}[1] = 0$  by symmetry, and

$$\left(\frac{1}{2}I + A_{H\nu}^{j,0}\right)[1] = \lambda_0 \quad (47)$$

where

$$\lambda_0 = \frac{1}{2} - \int_0^{2\pi} \left[ \frac{e^{-r^2(1-\cos s)/(2\Delta t)}}{4\pi} - \frac{(1-\cos s)r^2 E_1\left(\frac{r^2(1-\cos s)}{2\Delta t}\right)}{8\pi\Delta t} \right] ds. \quad (48)$$

Since  $E_1(x) > 0$  for  $x > 0$ , we have  $\lambda_0 > 0$  for any  $r > 0$  and  $\Delta t > 0$ . Thus, the system (43) has eigenvalues 0 and  $\lambda_0$  with eigenvectors  $[1 \ 0]^T$  and  $[0 \ 1]^T$ .

For  $k \neq 0$ , we have

$$\begin{aligned} \left(\frac{1}{2}I + S_{L\nu}\right)[e^{iks}](s') &= \frac{1}{2}e^{iks'}, \\ S_{L\tau}[e^{iks}](s') &= -\frac{1}{2}H[e^{iks}](s') = \frac{1}{2}i \operatorname{sgn}(k)e^{iks'}, \\ \left(\frac{1}{2}I + A_{H\nu}^{j,0}\right)[e^{iks}](s') &= a_k e^{iks'}, \\ A_{H\tau}^{j,0}[e^{iks}](s') &= b_k e^{iks'}, \end{aligned} \quad (49)$$



with  $a_k, b_k$  defined by the formulas

$$\begin{aligned}
a_k &= \frac{1}{2} - \frac{1}{4\pi} \int_{-\pi}^{\pi} e^{-\frac{r^2 \sin^2(s/2)}{\Delta t}} \cos(ks) ds \\
&\quad + \frac{r^2}{8\pi\Delta t} \int_{-\pi}^{\pi} (1 - \cos s) E_1\left(\frac{r^2 \sin^2(s/2)}{\Delta t}\right) \cos(ks) ds, \\
b_k &= \frac{i}{4\pi} \int_{-\pi}^{\pi} \cot\left(\frac{s}{2}\right) e^{-\frac{r^2 \sin^2(s/2)}{\Delta t}} \sin(ks) ds \\
&\quad - \frac{ir^2}{8\pi\Delta t} \int_{-\pi}^{\pi} \sin(s) E_1\left(\frac{r^2 \sin^2(s/2)}{\Delta t}\right) \sin(ks) ds.
\end{aligned} \tag{50}$$

We note that  $E_1(x)$  has a series expansion  $E_1(x) = \ln x + \gamma + x + \frac{x^2}{4} + \dots$  and that the spectrum of an integral operator with a smooth kernel decays exponentially fast. Thus, we have

$$\begin{aligned}
a_k &\approx \frac{1}{2} + \frac{r^2}{8\pi\Delta t} \int_{-\pi}^{\pi} (1 - \cos s) \ln(\sin^2(s/2)) \cos(ks) ds, \\
b_k &\approx \frac{i}{4\pi} \int_{-\pi}^{\pi} \cot\left(\frac{s}{2}\right) \sin(ks) ds \\
&\quad - \frac{ir^2}{8\pi\Delta t} \int_{-\pi}^{\pi} \sin(s) \ln(\sin^2(s/2)) \sin(ks) ds.
\end{aligned} \tag{51}$$

Using the facts (see, for example, [35]) that

$$\int_{-\pi}^{\pi} \ln(\sin^2(s/2)) \cos(ks) ds = -\frac{2\pi}{|k|}, \quad \frac{1}{2\pi} \int_{-\pi}^{\pi} \cot\left(\frac{s}{2}\right) \sin(ks) ds = \operatorname{sgn}(k),$$

we obtain

$$a_k \approx \frac{1}{2} - \frac{r^2}{4\Delta t|k|^3}, \quad b_k \approx \frac{i}{2} \operatorname{sgn}(k) - \frac{ir^2}{4\Delta tk^2} \operatorname{sgn}(k). \tag{52}$$

Combining all the above, we see that for the Fourier mode  $e^{iks}$  with  $k$  large, the following  $2 \times 2$  matrix determines its spectral behavior:

$$\begin{bmatrix} \frac{1}{2} & \frac{i}{2} \operatorname{sgn}(k) \left[1 - \frac{r^2}{2\Delta tk^2}\right] \\ -\frac{i}{2} \operatorname{sgn}(k) & \frac{1}{2} \end{bmatrix}. \tag{53}$$

The above matrix has roughly equal eigenvalues and singular values with  $\lambda_{k1} \approx \sigma_{k1} \approx 1 - \frac{r^2}{8\Delta tk^2}$  and  $\lambda_{k2} \approx \sigma_{k2} \approx \frac{r^2}{8\Delta tk^2}$  for  $k$  large. In summary, the integral equation system (37) has eigenvalues (and roughly equal singular

values)  $0, \lambda_0, \frac{r^2}{8\Delta tk^2}, 1 - \frac{r^2}{8\Delta tk^2}$  for  $k$  large. From this, in the complement of the one-dimensional nullspace, the condition number of the linear system can be seen to be of the order  $O(\Delta t/h^2)$  with  $h = 2\pi/N$  the spatial discretization size, assuming a uniform grid (so that  $k \approx N \approx 1/h$ ). In short, the condition number is  $O(N)$  for  $\Delta t = O(h)$  and  $O(1)$  for  $\Delta t = O(h^2)$ . For a fixed time step  $\Delta t$  independent of  $N$ , the condition number is  $O(N^2)$  (see fig. 1). These estimates are essentially the same as the conditioning of an implicit finite difference approximation applied to the heat equation with the same  $\Delta t$  and  $h$ .

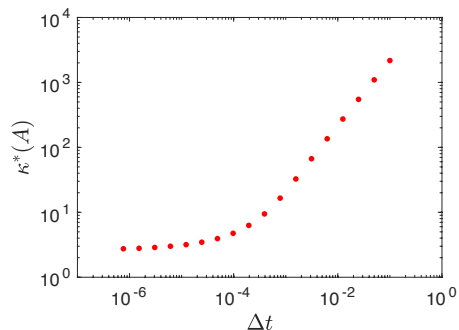


Figure 1: The condition number of the fully implicit combined source integral equation (in the complement of the one-dimensional nullspace) as a function of the time step for a circle of radius  $r = 0.6$ , discretized with 128 points.

The preceding analysis can be extended, in part, to the case of an arbitrary smooth curve.

**Lemma 5** *The nullspace of the system of integral equations (37) contains functions of the form  $[\rho_0(\mathbf{x})f(t) \ 0]^T$  where  $\rho_0(\mathbf{x})$  spans the one-dimensional nullspace of the operator  $\frac{1}{2}I + S_{L\nu}$  and  $f(t)$  an arbitrary smooth function on  $[0, T]$ .*

*Proof:* It is well known that the operator  $\frac{1}{2}I + S_{L\nu}$  has a one-dimensional nullspace (see, for example, [36]). Let us denote a corresponding null vector by  $\rho_0$ . It is easy to see that the function  $v = S_L[\rho_0]$  solves the interior Neumann problem for the Laplace equation with zero boundary data. From well-known properties of harmonic functions, this implies that  $v$  must be constant in  $D$ , so that its tangential derivative must be zero on the boundary. Thus,  $S_{L\tau}[\rho_0] = 0$ , completing the proof.  $\square$

**Remark 4** *Numerical experiments indicate that the only null vectors of (37) are the functions identified in (5). We conjecture that the coupled system of integral equations is exactly rank one deficient in any simply connected domain.*

## 5 Numerical results for the coupled integral equation system

Let us first consider the behavior of the implicit, second-order accurate one-step marching scheme described above. We will refer to solving the resulting system of the form (43) as the fully implicit combined source integral equation (FI-CSIE). As discussed in section 3.2, we use a 16th order accurate spatial quadrature rule [1] so that the spatial error is negligible and we accelerate the computation of the history part using the Fourier spectral method of [28, 34].

In fig. 2, we plot the eigenvalues of the system matrix with  $n = 64$  and  $n = 128$ , respectively, when  $\Gamma$  is a circle of radius  $r = 0.6$ . Note that the asymptotic analysis is in close agreement with direct discretization. It is

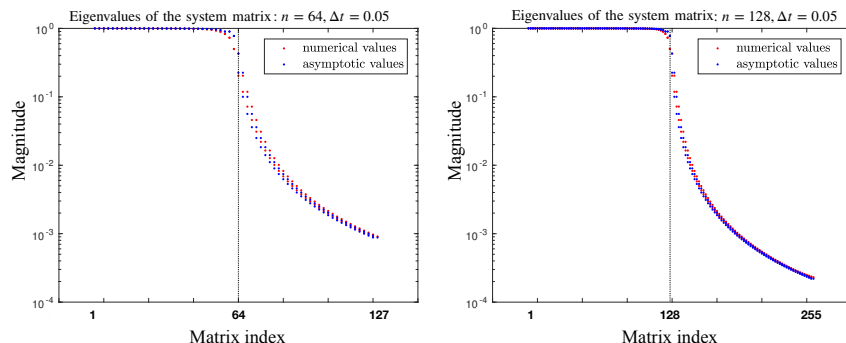


Figure 2: Magnitude of the eigenvalues of the system matrix (of size  $2n$ ) for a circle of radius  $r = 0.6$ , discretized with  $n$  points. The red dots are numerical values and the blue dots are the asymptotic values from section 4. The  $x$ -axis corresponds to the eigenvalue index, plotted in decreasing order. The eigenvalues from the asymptotic analysis are ordered in the corresponding fashion. We omit the exact zero eigenvalue from the Fourier analysis, which is manifested by a single eigenvalue of order  $10^{-15}$  in the matrix analysis.

worth noting that a physical constraint on the boundary data  $\mathbf{g}$  or  $\tilde{\mathbf{g}}$  is that the normal component integrates to zero on  $\Gamma$ . Such data has no projection

onto the nullvector of the system matrix so that an iterative method such as GMRES can be applied without any modification. With a stopping criterion for the residual set to  $10^{-12}$ , tables 1 and 2 show the performance of GMRES and the obtained error when the boundary is either an ellipse with aspect ratio 2 : 1 or a smooth hexagram, respectively (fig. 3). For all the tables presented in this paper, we take as the exact solution the divergence-free velocity field

$$\begin{aligned} \mathbf{u}(\mathbf{x}, t) = & \sum_{j=1}^{10} \sum_{k=0}^{\lfloor t/(2h) \rfloor} \frac{(x_2 - x_{2j}, x_{1j} - x_1)}{|\mathbf{x} - \mathbf{x}_j|^2} \left( e^{-\frac{|\mathbf{x} - \mathbf{x}_j|^2}{4(t - (2k+1)h)}} - e^{-\frac{|\mathbf{x} - \mathbf{x}_j|^2}{4(t - (2k+2)h)}} \right) \\ & + t \cos(313\pi t)(x_1, -x_2) + \frac{t^2}{4} \cos(233\pi t)e^{x_1}(\cos x_2, -\sin x_2) \\ & + 2t \sin(299\pi t)e^{x_2}(\cos x_1, \sin x_1), \end{aligned} \quad (54)$$

where  $h = 0.1$ ,  $\mathbf{x} = (x_1, x_2)$  and the  $\{\mathbf{x}_j\}$  are chosen to be equispaced on the unit circle, which encloses both domains of interest. 96 points are used to discretize the ellipse and 160 points are used to discretize the hexagram. In both tables, the first column lists the total number of time steps  $N$  needed to reach  $t = 1$ ; the second column lists the time step; the third column lists the average number of GMRES iterations required to solve the system to the desired tolerance; the fourth column lists the relative  $l_2$  error at 20 random points in the computational domain; the last column lists the ratio of the errors for each doubling of  $N$ . Note that the data are consistent with second order accuracy in time. Note also that the number of iterations is approximately equal to the number of points on the boundary, as expected for a large time step with  $\Delta t \approx 1/N$ .

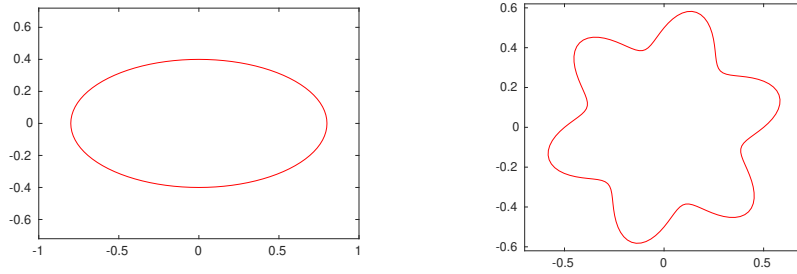


Figure 3: Boundary curves for tables 1 and 2, respectively.

**Table 1: Numerical results for the ellipse using the second order accurate fully implicit marching scheme. The matrix size is  $192 \times 192$ .**

$N$	$\Delta t$	$N_{\text{its}}$	Error	Ratio
10	1/10	93	$2.0 \cdot 10^{-2}$	
20	1/20	93	$1.2 \cdot 10^{-2}$	1.6
40	1/40	92	$3.8 \cdot 10^{-3}$	3.8
80	1/80	90	$7.5 \cdot 10^{-4}$	4.2
160	1/160	86	$1.8 \cdot 10^{-4}$	4.1

**Table 2: Numerical results for the hexagram using the second order accurate fully implicit marching scheme. The matrix size is  $320 \times 320$ .**

$N$	$\Delta t$	$N_{\text{its}}$	Error	Ratio
10	1/10	172	$1.8 \cdot 10^{-2}$	
20	1/20	178	$6.9 \cdot 10^{-3}$	2.6
40	1/40	183	$1.5 \cdot 10^{-3}$	4.5
80	1/80	185	$2.8 \cdot 10^{-4}$	5.5
160	1/160	183	$6.1 \cdot 10^{-5}$	4.6

## 6 The predictor corrector combined source integral equation (PC-CSIE)

The previous section shows that the fully implicit combined source integral equation (FI-CSIE) yields a somewhat ill-conditioned system of equations for large time steps. We now investigate a method for solving the unsteady Stokes equations using a rule of predictor-corrector type.

**Definition 6** *The  $k$ th order predictor-corrector scheme for the CSIE, denoted by PC-CSIE( $k$ ), is given by*

Step 1 : Set  $\mu_j = P_k^E[\boldsymbol{\mu}_{j-1}](j\Delta t)$ ,

Step 2 : Solve  $\left(\frac{1}{2}I + \mathcal{S}_{L\nu}\right) \rho_j = \nu \cdot \tilde{\mathbf{g}} + \mathcal{S}_{H\tau}^{\text{far}}[\boldsymbol{\mu}_{j-1}] + \mathcal{S}_{H\tau}^{\text{loc}}[\boldsymbol{\mu}_j]$ ,

Step 3 : Solve  $\left(\frac{1}{2}I + A_{H\nu}^{j,0}\right) \mu_j = \tau \cdot \tilde{\mathbf{g}} - \mathcal{S}_{H\nu}^{\text{far}}[\boldsymbol{\mu}_{j-1}] - F_{H\nu}^{j,k}[\boldsymbol{\mu}_{j-1}] - \mathcal{S}_{L\tau}[\rho_j]$ ,

using the notation of section 3.2.

That is, we first extrapolate  $\mu_j$  from previous time steps, then solve for  $\rho_j$ , and finally solve for  $\mu_j$  given the newly computed  $\rho_j$ . Note that the integral equation in step 2 of PC-CSIE( $k$ ) is a Fredholm equation of the second kind. While it has a one-dimensional nullspace, it is simply the classical equation for the harmonic interior Neumann problem obtained when representing the solution as a single layer potential. Since the right-hand side is compatible, the resulting linear system is easily solved using GMRES with  $O(1)$  iterations. The integral equation in step 3 is a Volterra equation of the second kind. It is always invertible and well-conditioned (at least on smooth curves).

The obvious difference between PC-CSIE ( $k$ ) and the fully implicit version comes from the extrapolation step. While the order of accuracy can be arbitrarily high, and the individual integral equations are well-conditioned, the stability of the resulting scheme remains to be studied.

Preliminary experiments suggest that the schemes PC-CSIE(2) and PC-CSIE(3) are stable even for moderately large time steps, while PC-CSIE(4) is not, but a thorough analysis remains to be undertaken (see section 8). Using the same geometries as above (fig. 3), we obtain the results in Table 3 for the ellipse (top) and the hexagram (bottom). Note that many fewer GMRES iterations are required for each step. The convergence rates, estimated by the error ratios in the last column are somewhat erratic, but generally better than the theoretical estimate  $2^k$ .

## 7 High order schemes using spectral deferred corrections

Instead of seeking to develop stable higher order predictor-corrector type schemes, we now show that more rapid convergence is easily achieved by combining PC-CSIE(2) with spectral deferred correction (SDC) [7, 16, 29, 43].

A very brief introduction to deferred corrections follows: suppose that we seek the solution  $v(t)$  of some time-dependent problem starting at  $t = 0$ , and that an approximate solution can be computed for  $k$  steps on  $[0, \Delta t]$  using a low order accurate method, with an error of the order  $O(\Delta t^m)$  for some  $m < k$ . We denote the discrete solution at those  $k$  points by  $\mathbf{v}_k^{[0]}$ . One can then interpolate the low order solution by a polynomial in  $t$  of order  $k$ , namely  $P_k^I[\mathbf{v}_k^{[0]}]$ , defined in section 3.2. This allows us to define a continuous error function

$$\delta^{[0]}(t) = v(t) - P_k^I[\mathbf{v}_k^{[0]}](t),$$

**Table 3: Numerical results for the ellipse and hexagram using the PC-CSIE(2) method. The matrix size is  $96 \times 96$  for the ellipse and  $256 \times 256$  for the hexagram at each stage.**

Ellipse				
$N$	$\Delta t$	$N_{\text{its}}$	Error	Ratio
80	1/40	7	$4.2 \cdot 10^{-2}$	
160	1/80	7	$1.7 \cdot 10^{-3}$	24
320	1/160	7	$2.9 \cdot 10^{-4}$	6.0
640	1/320	7	$4.8 \cdot 10^{-5}$	6.0
1280	1/640	7	$9.0 \cdot 10^{-6}$	5.3
Hexagram				
$N$	$\Delta t$	$N_{\text{its}}$	Error	Ratio
80	1/40	12	$9.6 \cdot 10^{-3}$	
160	1/80	12	$3.6 \cdot 10^{-3}$	2.7
320	1/160	11	$5.8 \cdot 10^{-4}$	6.1
640	1/320	11	$9.9 \cdot 10^{-5}$	5.8
1280	1/640	11	$1.7 \cdot 10^{-5}$	5.7

which can be substituted into the governing equation for  $v(t)$  and solved for  $\delta^{[0]}(t)$ , using the same low order scheme. This generates the discrete solution vector  $\delta_k^{[0]}$ . A corrected approximation is then defined by

$$\mathbf{v}_k^{[1]} = \mathbf{v}_k^{[0]} + \delta_k^{[0]}.$$

It is straightforward to show that the error in  $\mathbf{v}_k^{[1]}$  is of the order  $O(h^{2m})$ , so long as  $2m < k$  and all computations involving the known function  $P_k^I[\mathbf{v}_k^{[0]}](t)$  are carried out with  $k$ th order accuracy. For further details, see the references above and [6]. The correction procedure is easily iterated until  $k$ th order accuracy is achieved. The process can then be repeated on the next time interval  $[\Delta t, 2\Delta t]$ , etc. (The phrase *spectral deferred correction* is typically used when the underlying problem has been formulated as an integral equation and the  $k$  stages are chosen at nodes corresponding to some high order spectral discretization, typically of Gauss or Gauss-Radau type.)

In the present context, let us assume that we have divided  $[0, T]$  into  $N$  equal subintervals  $[t_{i-1}, t_i]$  with  $t_i = i\Delta t$ ,  $\Delta t = T/N$  for  $i = 1, \dots, N$ . We restrict our attention to the  $i$ th such interval  $[t_{i-1}, t_i]$  which we will denote

by  $[\alpha, \beta]$  when the context is clear. Given a positive integer  $k$ , we will denote by  $\alpha < \tau_1, \dots, \tau_k = \beta$  the  $k$  Gauss-Radau nodes shifted and scaled to the interval  $[\alpha, \beta]$  (see, for example, [22]), with  $\tau_0 = \alpha$ . Let us denote the values of the densities  $\rho$  and  $\mu$  at these nodes by  $\boldsymbol{\rho}_k = (\rho_0, \rho_1, \dots, \rho_k)^T$  and  $\boldsymbol{\mu}_k = (\mu_0, \mu_1, \dots, \mu_k)^T$ , respectively. Since we are discretizing in time only, recall that  $\rho_i, \mu_i$  are functions of the spatial variable  $\mathbf{y} \in \Gamma(t)$ .

Following the principle outlined above, the first step of SDC for the mixed potential formulation is to use some low order scheme to obtain  $\boldsymbol{\rho}_k^{[0]}$  and  $\boldsymbol{\mu}_k^{[0]}$ . We then use these two vectors to obtain interpolating polynomials of degree  $k - 1$  in time, namely  $P_k^I[\boldsymbol{\mu}_k^{[0]}]$  and  $P_k^I[\boldsymbol{\rho}_k^{[0]}]$  and define

$$\delta_\mu^{[0]}(t) = \mu(t) - P_k^I[\boldsymbol{\mu}_k^{[0]}], \quad \delta_\rho^{[0]}(t) = \rho(t) - P_k^I[\boldsymbol{\rho}_k^{[0]}].$$

Inserting this representation into eq. (37), we obtain

$$\begin{aligned} \frac{1}{2}\delta_\rho^{[0]}(\mathbf{x}, t) + \mathcal{S}_{L\nu}[\delta_\rho^{[0]}](\mathbf{x}, t) + \mathcal{S}_{H\tau}[\delta_\mu^{[0]}](\mathbf{x}, t) &= R_1(\mathbf{x}, t), \\ -\mathcal{S}_{L\tau}[\delta_\rho^{[0]}](\mathbf{x}, t) + \frac{1}{2}\delta_\mu^{[0]}(\mathbf{x}, t) + \mathcal{S}_{H\nu}[\delta_\mu^{[0]}](\mathbf{x}, t) &= R_2(\mathbf{x}, t), \end{aligned} \quad (55)$$

where the residuals  $R_1$  and  $R_2$  are given by

$$\begin{aligned} R_1(\mathbf{x}, t) &= \nu \cdot \tilde{\mathbf{g}}(\mathbf{x}, t) - \frac{1}{2}P_k^I[\boldsymbol{\rho}_k^{[0]}](\mathbf{x}, t) - \mathcal{S}_{L\nu}[P_k^I[\boldsymbol{\rho}_k^{[0]}]](\mathbf{x}, t) - \mathcal{S}_{H\tau}[P_k^I[\boldsymbol{\mu}_k^{[0]}]](\mathbf{x}, t), \\ R_2(\mathbf{x}, t) &= -\tau \cdot \tilde{\mathbf{g}}(\mathbf{x}, t) + \mathcal{S}_{L\tau}[P_k^I[\boldsymbol{\rho}_k^{[0]}]](\mathbf{x}, t) - \frac{1}{2}P_k^I[\boldsymbol{\mu}_k^{[0]}](\mathbf{x}, t) - \mathcal{S}_{H\nu}[P_k^I[\boldsymbol{\mu}_k^{[0]}]](\mathbf{x}, t). \end{aligned}$$

Note that this is exactly the same equation as (37), but with a different right-hand side. Since, as noted above, SDC requires that all residuals be computed with high order accuracy, we have provided some of the integrals needed at the intermediate stages in the Appendix.

After solving eq. (55) at the same  $k$  stages, yielding  $[\delta_\rho^{[0]}]_k, [\delta_\mu^{[0]}]_k$ , we let

$$\boldsymbol{\rho}_k^{[1]} = \boldsymbol{\rho}_k^{[0]} + [\delta_\rho^{[0]}]_k, \quad \boldsymbol{\mu}_k^{[1]} = \boldsymbol{\mu}_k^{[0]} + [\delta_\mu^{[0]}]_k. \quad (56)$$

This procedure may be repeated until the desired order of accuracy is achieved.

We have implemented SDC using the second order predictor corrector scheme PC-CSIE(2) described in the previous section. For simplicity, we provide numerical results in table 4 for the case of a circle. In this table,  $\text{SDC}_k^j$  denotes the scheme with  $k$  Gauss-Radau nodes on each subinterval and  $j$  iterations of deferred correction. In particular,  $\text{SDC}_k^0$  is simply the



uncorrected solution obtained with PC-CSIE(2).  $N$  is the number of subintervals,  $\Delta t$  is the time step size for each subinterval,  $E$  is the relative  $l^2$  error for the method indicated in the subscript, and  $N_{\text{it}}$  is the average number of iterations for GMRES to reach the requested tolerance  $10^{-12}$ . The total number of time steps is  $Nk$  and the expected error reduction should be  $2^{2(j+1)}$  for  $\text{SDC}_k^j$  until  $2(j+1) > k$ , since we are driving the deferred correction process with a second order accurate scheme. While the behav-

**Table 4: Numerical results for the circle of radius 0.5, using spectral deferred correction. The number of points in the spatial discretization is 200.**

$Nk$	$\Delta t/k$	$N_{\text{its}}$	$E_{\text{SDC}_5^0}$	$E_{\text{SDC}_5^1}$	$E_{\text{SDC}_5^2}$	$E_{\text{SDC}_5^3}$	$E_{\text{SDC}_5^4}$
40	1/20	2.7	$1.5 \cdot 10^{-2}$	$2.5 \cdot 10^{-2}$	$2.5 \cdot 10^{-2}$	$2.5 \cdot 10^{-2}$	$2.5 \cdot 10^{-2}$
80	1/40	2.6	$3.0 \cdot 10^{-3}$	$3.5 \cdot 10^{-5}$	$1.8 \cdot 10^{-4}$	$1.8 \cdot 10^{-4}$	$1.8 \cdot 10^{-4}$
160	1/80	2.7	$2.7 \cdot 10^{-3}$	$3.8 \cdot 10^{-5}$	$3.7 \cdot 10^{-5}$	$3.7 \cdot 10^{-5}$	$3.7 \cdot 10^{-5}$
320	1/160	2.6	$6.9 \cdot 10^{-4}$	$1.5 \cdot 10^{-7}$	$1.3 \cdot 10^{-7}$	$9.8 \cdot 10^{-8}$	$4.5 \cdot 10^{-8}$
640	1/320	2.6	$1.6 \cdot 10^{-4}$	$1.1 \cdot 10^{-8}$	$5.3 \cdot 10^{-9}$	$4.5 \cdot 10^{-9}$	$4.9 \cdot 10^{-9}$

ior of the SDC schemes as a function of the number of correction sweeps is somewhat erratic, it is more or less consistent with the asymptotic estimates. That is,  $\text{SDC}_5^0$  converges approximately like a second order scheme, while  $\text{SDC}_5^1$  converges at a much higher rate. Further sweeps of deferred correction don't increase the convergence rate significantly, since the degree of polynomial approximation is only four, limiting the order of accuracy, as discussed above. Note, however, that these further sweeps have no impact on stability.

**Remark 5** *A nice feature of the mixed potential representation is the complete separation of the instantaneous pressure source from the vortex source. As a result, even though the exact solution defined in eq. (54) has a highly oscillatory pressure field, the numerical results in tables 1 to 4 show that high accuracy is achieved even for large time steps that under-resolve the oscillatory behavior of the pressure.*

## 8 Conclusions and future work

We have developed a new integral representation for the unsteady Stokes equations which makes use of simple harmonic and heat potentials, leading to the *combined source integral equation* (CSIE). Unlike schemes based

on the unsteady Stokeslet [34], this permits the direct application of well-developed fast algorithms (see, for example, [26, 28, 41, 48, 52, 53] and [11, 20, 25, 27, 38, 42]).

While the fully coupled CSIE is not of Fredholm type, we have shown that each individual equation is well-conditioned, and found that a second-order predictor-corrector type method is effective even for large time steps. Moreover, one can achieve high order accuracy through the use of spectral deferred correction. Since our primary goal in the present paper is the development of the mathematical representation itself, a more thorough investigation of various predictor-corrector, Runge-Kutta, and implicit-explicit type marching schemes will be carried out at a later date.

It is worth noting that the mixed potential representation and existing gauge methods (see eq. (6)) bear some resemblance. The principle differences are (1) that we are working in an integral equation-based framework, (2) that we apply the Helmholtz decomposition to the inhomogeneous data rather than to the auxiliary unknown vector field  $\mathbf{m}$ , and (3) that we have as unknowns only the vortex source and pressure source, which are restricted to the boundary and for which imposing velocity boundary conditions is straightforward.

A number of open questions remain, including the completeness of the representation for multiply-connected domain, a detailed characterization of the nullspace of the coupled system, and the extension of the mixed potential formulation to other boundary/interface conditions. While our representation is formally valid in either fixed or moving geometries, we have not yet investigated its performance in the nonstationary case. To solve the equations with a forcing term (or the full Navier-Stokes equations), we also need to couple the solver described here with volume-integral based codes for the Helmholtz decomposition, as discussed in section 2.3. We are presently investigating all of these topics and will report on our progress at a later date.

## Appendix

For the SDC method of section 7, using product integration in time as in [34], the residual is required at intermediate stage  $\tau_i \in [\alpha, \beta]$ . This involves integrals beyond those given by eq. (4.9) in [34]. We provide those integrals here, which are sufficient to obtain fourth order accuracy.

$$\begin{aligned}
& \int_{\alpha}^{\alpha+\tau_i} e^{-r^2/4(\alpha+\tau_i-\tau)} \frac{(\beta-\tau)^j}{(\alpha+\tau_i-\tau)^2} d\tau \\
&= \begin{cases} \frac{4}{r^2} e^{-c}, & j=0, \\ E_1(c) + \frac{b}{a} e^{-c}, & j=1, \\ \left(\tau_i + \frac{b^2}{a}\right) e^{-c} - E_1(c)(a-2b), & j=2, \\ -\frac{e^{-c}}{2} (\tau_i a - x_i^2 - 6\tau_i b - 2b^3/a) + E_1(c)(a^2 - 6ab + 6b^2), & j=3, \\ \frac{e^{-c}}{6} (2\tau_i^3 - \tau_i^2(a-12b) + \tau_i(a-6b)^2 + 6b^4/a) \\ - \frac{E_1(c)}{6} (a^3 - 12a^2b + 36ab^2 - 24b^3), & j=4, \end{cases} \\
& \hspace{15em} (57)
\end{aligned}$$

where  $r = \|\mathbf{x} - \mathbf{y}\|$ ,  $c = \frac{r^2}{4\tau_i}$ ,  $a = \frac{r^2}{4}$ ,  $b = \Delta t - \tau_i$ .

## Acknowledgments

We would like to thank Alex Barnett, Charlie Epstein, Jingfang Huang, Manas Rachh, Shravan Veerapaneni and Jun Wang for many useful conversations.

## References

- [1] B. K. ALPERT, *Hybrid Gauss-trapezoidal quadrature rules*, SIAM J. Sci. Comput., 20 (1999), pp. 1551–1584.
- [2] C. R. ANDERSON, *Vorticity boundary conditions and boundary vorticity generation for two-dimensional incompressible flows*, J. Comput. Phys., 80 (1989), pp. 72–97.
- [3] R. ARIS, *Vectors, tensors, and the basic equations of fluid mechanics*, Prentice-Hall, Englewood Cliffs, NJ, 1962.
- [4] M. BEN-ARTZI, J.-P. CROISILLE, D. FISHELOV, AND S. TRACHTENBERG, *A pure-compact scheme for the streamfunction formulation of the Navier-Stokes equations*, J. Comput. Phys., 205 (2005), pp. 640–664.

- [5] M. BEN-ARTZI, D. FISHELOV, AND S. TRACHTENBERG, *Vorticity dynamics and numerical resolution of Navier-Stokes equations*, Math. Model. Numer. Anal., 35 (2001), pp. 313–330.
- [6] K. BÖHMER AND E. H. J. STETTER, *Defect Correction Methods, Theory and Applications*, Springer-Verlag, New York, 1984.
- [7] A. BOURLIOUX, A. T. LAYTON, AND M. L. MINION, *High-order multi-implicit spectral deferred correction methods for problems of reactive flow*, J. Comput. Phys., 189 (2003), pp. 651–675.
- [8] J. BREMER AND Z. GIMBUTAS, *A Nyström method for weakly singular integral operators on surfaces*, J. Comput. Phys., 231 (2012), pp. 4885–4903.
- [9] D. L. BROWN, R. CORTEZ, AND M. L. MINION, *Accurate projection methods for the incompressible Navier-Stokes equations*, J. Comput. Phys., 168 (2001), pp. 464–499.
- [10] T. F. BUTTKE, *Velocity methods: Lagrangian numerical methods which preserve the Hamiltonian structure of incompressible fluid flow*, in Vortex Flows and Related Numerical Methods, 1993, pp. 39–57.
- [11] H. CHENG, L. GREENGARD, AND V. ROKHLIN, *A fast adaptive multipole algorithm in three dimensions*, J. Comput. Phys., 155 (1999), pp. 468–498.
- [12] A. J. CHORIN, *Numerical solution of the Navier-Stokes equations*, Math. Comput., 22 (1968), pp. 745–762.
- [13] D. COLTON AND R. KRESS, *Inverse Acoustic and Electromagnetic Scattering Theory*, Springer, New York, NY, 2012.
- [14] R. CORTEZ, *On the accuracy of impulse methods for fluid flow*, SIAM J. Sci. Comput., 19 (1998), pp. 1290–1302.
- [15] E. J. DEAN, R. GLOWINSKI, AND O. PIRONNEAU, *Iterative solution of the stream function-vorticity formulation of the Stokes problem, application to the numerical simulation of incompressible viscous flow*, Comput. Method Appl. Mech. Engrg., 87 (1991), pp. 117–155.
- [16] A. DUTT, L. GREENGARD, AND V. ROKHLIN, *Spectral deferred correction methods for ordinary differential equations*, BIT, 40 (2000), pp. 241–266.

- [17] W. E AND J.-G. LIU, *Vorticity boundary condition and related issues for finite difference scheme*, J. Comput. Phys., 124 (1996), pp. 368–382.
- [18] ———, *Finite difference methods for 3-d viscous incompressible flows in the vorticity-vector potential formulation on nonstaggered grids*, J. Comput. Phys., 138 (1997), pp. 57–82.
- [19] ———, *Gauge method for viscous incompressible flows*, Comm. Math. Sci., 1 (2003), pp. 317–332.
- [20] F. ETHRIDGE AND L. GREENGARD, *A new fast-multipole accelerated Poisson solver in two dimensions*, SIAM J. Sci. Comput., 23 (2001), pp. 741–760.
- [21] E. FABES, M. JODEIT, AND N. RIVIÉRE, *Potential theoretic techniques for boundary value problems on  $C^1$  domains*, Acta Math., 141 (1978), pp. 165–186.
- [22] W. GAUTSCHI, *GaussRadau formulae for Jacobi and Laguerre weight functions*, Math. Comput. Simul., 54 (2000), pp. 403–412.
- [23] V. GIRAULT AND P. A. RAVIART, *Finite element methods for Navier-Stokes equations*, vol. 5 of Springer Series in Computational Mathematics, Springer-Verlag, Berlin, 1986.
- [24] L. GREENGARD AND M. KROPINSKI, *An integral equation approach to the incompressible Navier-Stokes equations in two-dimensions*, SIAM J. Sci. Comput., 20 (1998), pp. 318–336.
- [25] L. GREENGARD AND J.-Y. LEE, *A direct adaptive Poisson solver of arbitrary order accuracy*, J. Comput. Phys., 125 (1996), pp. 415–424.
- [26] L. GREENGARD AND P. LIN, *Spectral approximation of the free-space heat kernel*, Appl. Comput. Harmon. Anal., 9 (2000), pp. 83–97.
- [27] L. GREENGARD AND V. ROKHLIN, *A fast algorithm for particle simulations*, J. Comput. Phys., 73 (1987), pp. 325–348.
- [28] L. GREENGARD AND J. STRAIN, *A fast algorithm for the evaluation of heat potentials*, Comm. Pure Appl. Math., 43 (1990), pp. 949–963.
- [29] T. HAGSTROM AND R. ZHOU, *On the spectral deferred correction of splitting methods for initial value problems*, Comm. Appl. Math. Comput. Sci., 1 (2006), pp. 169–205.

- [30] S. HAO, A. H. BARNETT, P. G. MARTINSSON, AND P. YOUNG, *High-order accurate methods for Nyström discretization of integral equations on smooth curves in the plane*, Adv. Comput. Math., 40 (2014), pp. 245–272.
- [31] W. D. HENSHAW, *A fourth-order accurate method for the incompressible Navier-Stokes equations on overlapping grids*, J. Comput. Phys., 113 (1994), pp. 13–25.
- [32] T. Y. HOU AND B. R. WETTON, *Stable fourth-order stream-function methods for incompressible flows with boundaries*, J. Comput. Math., 27 (2009), pp. 441–458.
- [33] S. JIANG, M. C. A. KROPINSKI, AND B. QUAIFFE, *Second kind integral equation formulation for the modified biharmonic equation and its applications*, J. Comput. Phys., 249 (2013), pp. 113–126.
- [34] S. JIANG, S. VEERAPANENI, AND L. GREENGARD, *Integral equation methods for unsteady Stokes flow in two dimensions*, SIAM J. Sci. Comput., 34 (2012), pp. A2197–A2219.
- [35] P. KOLM, S. JIANG, AND V. ROKHLIN, *Quadruple and octuple layer potentials in two dimensions I: Analytical apparatus*, Appl. Comput. Harmon. Anal., 14 (2003), pp. 47–74.
- [36] R. KRESS, *Linear Integral Equations*, vol. 82 of Applied Mathematical Sciences, Springer–Verlag, Berlin, third ed., 2014.
- [37] O. A. LADYZHENSKAYA, *The Mathematical Theory of Viscous Incompressible Flow*, Gordon & Breach, New York, 1969.
- [38] H. M. LANGSTON, L. GREENGARD, AND D. ZORIN, *A free-space adaptive FMM-based PDE solver in three dimensions*, Comm. Appl. Math. Comput. Sci., 6 (2011), pp. 79–122.
- [39] J. LI AND L. GREENGARD, *High order accurate methods for the evaluation of layer heat potentials*, SIAM J. Sci. Comput., 31 (2009), pp. 3847–3860.
- [40] J.-G. LIU, J. LIU, AND R. L. PEGO, *Stable and accurate pressure approximation for unsteady incompressible viscous flow*, J. Comput. Phys., 229 (2010), pp. 3428–3453.

- [41] C. LUBICH AND R. SCHNEIDER, *Time discretization of parabolic boundary integral equations*, Numer. Math., 63 (1992), pp. 455–481.
- [42] D. MALHOTRA AND G. BIROS, *PVFMM: a parallel kernel independent FMM for particle and volume potentials*, Comm. Comput. Phys., 18 (2015), pp. 808–830.
- [43] M. L. MINION, *Semi-implicit projection methods for incompressible flow based on spectral deferred corrections*, Applied Numerical Mathematics, 48 (2004), pp. 369–387.
- [44] F. W. J. OLVER, D. W. LOZIER, R. F. BOISVERT, AND C. W. CLARK, eds., *NIST Handbook of Mathematical Functions*, Cambridge University Press, May 2010.
- [45] L. QUARTAPELLE, *Numerical solution of the incompressible Navier-Stokes equations*, Birkhauser Verlag, Basel, 1993.
- [46] R. SAYE, *Interfacial gauge methods for incompressible fluid dynamics*, Science Advances, 2 (2016), p. e1501869.
- [47] M. SIEGEL AND A.-K. TORNBORG, *A local target specific quadrature by expansion method for evaluation of layer potentials in 3D*, J. Comput. Phys., 364 (2018), pp. 365–392.
- [48] J. TAUSCH, *A fast method for solving the heat equation by layer potentials*, J. Comput. Phys., (2007).
- [49] R. TEMAM, *Sur l'approximation de la solution des equations de Navier-Stokes par la methode des fractionnaires II*, Arch. Rational Mech. Anal., 33 (1969), pp. 377–385.
- [50] G. VERCHOTA, *Layer potentials and boundary value problems for laplaces equation in lipschitz domains*, J. Funct. Anal., 59 (1984), pp. 572–611.
- [51] C. WANG AND J.-G. LIU, *Convergence of gauge method for incompressible flow*, Math. Comput., 69 (2000), pp. 1385–1407.
- [52] J. WANG AND L. GREENGARD, *An adaptive fast Gauss transform in two dimensions*, SIAM J. Sci. Comput., 40 (2018), pp. A1274–A1300.
- [53] J. WANG, L. GREENGARD, S. JIANG, AND S. K. VEERAPANENI, *A high-order solver for the two-dimensional heat equation in moving domains*, in preparation, (2018).